Available online at www.sciencedirect.com
ScienceDirect
Cement and Concrete Research 38 (2008) 487–499
Cement and Concrete Research

On the mechanism of polypropylene fibres in preventing fire spalling in self-compacting and high-performance cement paste

X. Liu [a,b,*], G. Ye [b,c], G. De Schutter [b], Y. Yuan [a], L. Taerwe [b]

[a] School of Civil Engineering, Tongji University, Shanghai, PR China
[b] Magnel Laboratory for Concrete Research, Department of Structural Engineering, Ghent University, Technologiepark-Zwijnaarde 904 B-9052, Ghent (Zwijnaarde), Belgium
[c] Microlab, Faculty of Civil Engineering and Geosciences, Delft University of Technology, Delft, The Netherlands

Received 17 January 2006; accepted 20 November 2007

Abstract

With the increasing application of self-compacting concrete (SCC) in construction and infrastructure, the fire spalling behavior of SCC has been attracting due attention. In high performance concrete (HPC), addition of polypropylene fibers (PP fibers) is widely used as an effective method to prevent explosive spalling. Hence, it would be useful to investigate whether the PP fibers are also efficient in SCC to avoid explosive spalling. However, no universal agreement exists concerning the fundamental mechanism of reducing the spalling risk by adding PP fiber. For SCC, the reduction of flowability should be considered when adding a significant amount of fibres.

In this investigation, both the micro-level and macro-level properties of pastes with different fiber contents were studied in order to investigate the role of PP fiber at elevated temperature in self-compacting cement paste samples. The micro properties were studied by backscattering electron microscopy (BSE) and mercury intrusion porosimetry (MIP) tests. The modification of the pore structure at elevated temperature was investigated as well as the morphology of the PP fibers. Some macro properties were measured, such as the gas permeability of self-compacting cement paste after heating at different temperatures. The factors influencing gas permeability were analyzed.

It is shown that with the melting of PP fiber, no significant increase in total pore volume is obtained. However, the connectivity of isolated pores increases, leading to an increase of gas permeability. With the increase of temperature, the addition of PP fibers reduces the damage of cement pastes, as seen from the total pore volume and the threshold pore diameter changes. From this investigation, it is concluded that the connectivity of pores as well as the creation of micro cracks are the major factors which determine the gas permeability after exposure to high temperatures. Furthermore, the connectivity of the pores acts as a dominant factor for temperatures below 300 °C. For higher temperatures micro cracks are becoming the major factor which influences the gas permeability.

Keywords: Cement paste; Microstructure; Gas permeability; PP fiber; Spalling

1. Introduction

Research on the explosive spalling of high performance concrete (HPC) has been carried out worldwide in the past decades. From the literature, most experiments on the spalling behaviour of concrete focused on structural elements, such as beams or columns [1–5]. Quite often, conclusions are based on analysis of the experimental results. The results are still a subject of debate, but there has been materials science based research on the spalling of concrete.

According to previous studies [6–9], spalling mainly depends on the temperature gradient and the increase in pore pressure in a concrete element at elevated temperature. The temperature gradient will cause thermal expansion gradient. So in this case, the thermal conductivity and thermal expansion are two influencing factors, which are determined by the concrete composition. Concerning the increase in pore pressure in concrete elements exposed to fire, different explanations can be forwarded. In general,

* Corresponding author. School of Civil Engineering, Tongji University, Shanghai, PR China. Tel.: +86 21 65980234; fax: +86 21 65984573.
E-mail address: xian.liu@tongji.edu.cn (X. Liu).

0008-8846/$ - see front matter © 2007 Elsevier Ltd. All rights reserved.
doi:10.1016/j.cemconres.2007.11.010

Table 1
Chemical composition of cement and limestone powder

	CEM I 52.5 (%)	Limestone filler (%)
CaO	63.95	–
SiO_2	20.29	0.80
Al_2O_3	4.52	0.17
Fe_2O_3	2.35	0.10
MgO	2.22	0.50
K_2O	0.94	–
Na_2O	0.20	–
SO_3	3.35	–
Cl^-	0.015	0.002
$CaCO_3$	–	98.00
C_3S	59.0	–
C_2S	12.60	–
C_3A	8.01	–
C_4AF	9.40	–

Table 3
Mix Proportions (in kg, unless stated otherwise)

	SCCP PPF0	SCCP PPF05	SCCP PPF1	HPCP PPF0	HPCP PPF05	HPCP PPF1
Portland cement CEM I 52.5	400	400	400	400	400	400
Water	165	165	165	132	132	132
Limestone powder	200	200	200	0	0	0
superplasticizer	3.2(l)	4.42(l)	5.55(l)	5	7	8.45
PP Fiber	0	0.5	1	0	0.5	1
Total powder content	600	600	600	400	400	400
Water/cement ratio	0.41	0.41	0.41	0.33	0.33	0.33
Water/powder ratio	0.28	0.28	0.28	0.33	0.33	0.33

pore pressure is related to the temperature, the moisture content, and the gas permeability. Up to now, only two instruments were reported to measure the pore pressure at elevated temperature [7,8,10]. However, the measured pore pressures were quite different in both cases.

Actually, addition of polypropylene (PP) fibers in concrete is considered as an effective method to prevent the spalling risk, and the investigation concerning its influence is still going on. For the mechanical and thermal properties of concrete containing PP fibers, the experimental results are not consistent, depending on the experimental program [11,12]. By measuring the pore pressure, Kalifa [7] found that the presence of fibres led to a large decrease in the pressure field that built up in the porous network during heating. On a statistical basis, Persson [13] suggested a content of 0.7kg/m^3 for indoor concrete and 1.4kg/m^3 for tunnel concrete, is sufficient to prevent explosive fire spalling in self-compacting concrete (SCC). Concerning the mechanism of PP fibers at elevated temperatures, most researchers state that melting fibers can create additional pores and small channels. Then moisture and vapor should be released more easily and correspondingly, pore pressure should decrease compared with concrete without PP fiber.

In comparison with large scale fire tests on structural elements, research at the material level seems to be more fundamental in investigating the spalling phenomenon when concrete is exposed to high temperatures. On the one hand, it seems that the addition of PP fiber would change the microstructural properties [8,12]. On the other hand, the macro properties are determined by the micro characteristics of the cementitious materials. For example, the permeability of concrete largely depends on its pore structure [14,15] and the mechanical properties can also be predicted by pore structure [16,17]. Bentz [18] once established a fiber-reinforced cement paste microstructural model to investigate PP fiber's action. This model was used to analyze the theoretical percolation threshold of PP fibers. As mentioned above, the pore pressure, which is closely connected to the pore structure, is one of the factors that influence the spalling of concrete. The parameters related to the pore structure, as used in existing spalling models [19–21], are either the total porosity or the threshold diameter. However, the influence of high temperatures on the pore structure itself is still not clear, neither the chemical changes nor physical changes.

Table 2
Characteristics of PP fiber

Density at solid state	0.93
Density at liquid state	0.85
Thickness (μm)	18
Width (μm)	150
Length (mm)	12
Melting temperature °C	171
Temperature at vaporization °C	341
Burning temperature °C	460
Thermal conductivity (w/m K)	0.15

In the past ten years, with excellent deformability, resistance to segregation and flow ability in heavily reinforced formwork without vibrators, SCC was widely used in construction and infrastructure. Recent research [22] has shown that at the same w/powder ratio, the porosity and pore size distribution of self-compacting concrete are very similar to those of high performance concrete. This means that when self-compacting concrete is exposed to elevated temperatures, it might have the same risk (i.e. explosive spalling) as high performance concrete. But the phase composition of SCC and HPC is different as observed by SEM and DTA/TGA measurements. In the case of limestone as filler in SCC concrete, the limestone particles are almost not decomposed up to a temperature of 700 °C and the weight loss of SCC is much smaller than that of HPC before this temperature [22].

This study aims to investigate the evolution of the chemical and physical properties of cement pastes and the change of macro properties caused by the microstructural changes at different elevated temperatures of self-compacting cement paste samples (SCCP). In the experiments, the samples were exposed to a predefined high temperature. After exposure, mercury intrusion porosimetry (MIP) and scanning electron microscopy (SEM) were applied to investigate the microstructure. Gas permeability tests were carried out in order to determine the effect of microstructural changes on the permeability of SCCP samples. Meanwhile, the influence of PP fiber was investigated. Different PP fiber dosages were used to compare both the micro

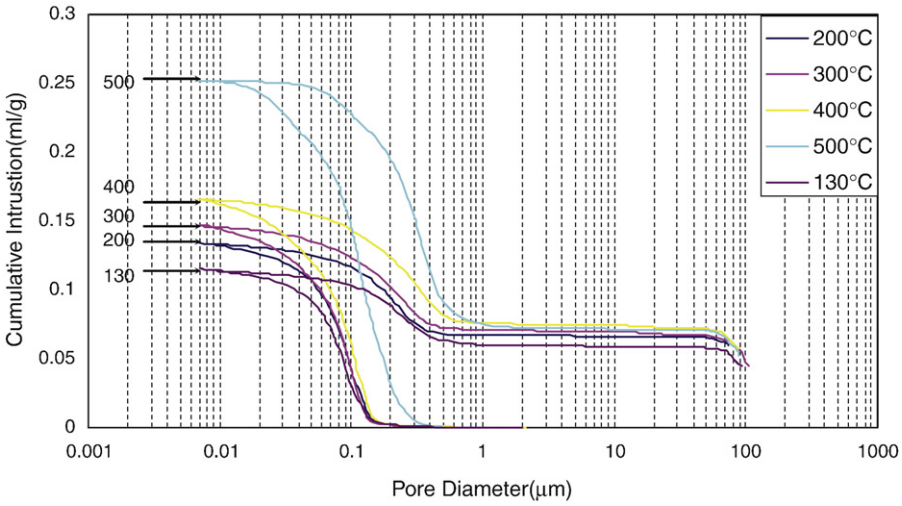

Fig. 1. Influence of temperature on pore volume of HPCP PPF0.

and macro properties. High-performance cement paste (HPCP) was studied as well, in comparison with SCCP.

2. Materials and methods

2.1. Materials and mixtures

The SCCP mixtures used in this study were prepared with Portland cement CEM I 52.5, with limestone powder added as filler. The limestone powder was produced from carboniferous limestone of a very high purity (98% of $CaCO_3$ content). The chemical composition of cement and limestone filler is given in Table 1.

The characteristics of the PP fibers used in this study are given in Table 2.

In the experimental programme, six mixtures including self-compacting cement paste (SCCP) and high performance cement paste (HPCP) were used. The PP fiber contents are 0, 0.5 and 1kg/m3 (or 0, 0.75, 1.5 percent by absolute volume content). The mix proportions of SCCP and HPCP with PP fibers at a dosage of 0, 0.5 and 1kg/m3 are listed in the Table 3.

During casting, the materials were first mixed with water for 2min at lower speed. Afterwards, the superplasticizer was added and the paste was mixed for another 3min at high speed. The specimens for the fire test were cast in a wooden mould with a size of 175×90×100mm. Four hours after casting, the samples were sealed with aluminium foils to prevent moisture loss, and the specimens were stored in a curing room at a temperature of 20 °C and a relative humidity of 60% for 28days.

2.2. Heating procedure

At a curing age of 28days, the samples were exposed at different target temperatures by using an electrical resistance furnace with a heating rate of 10 °C/min.

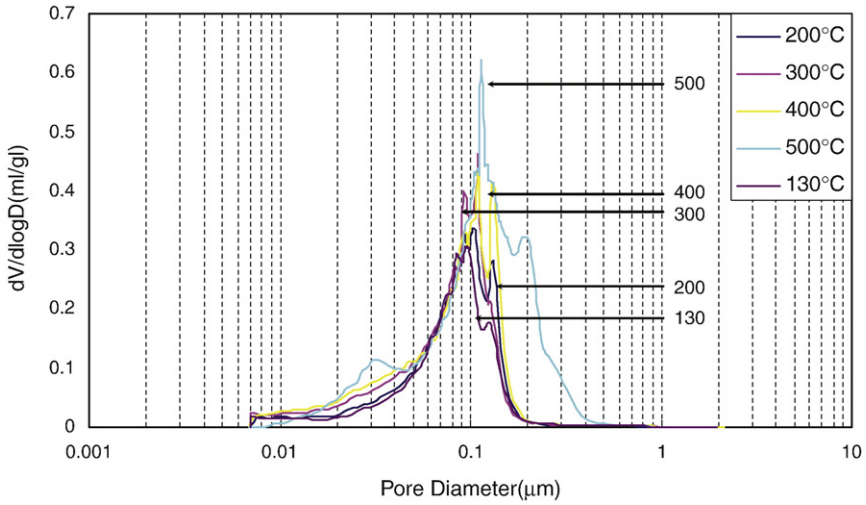

Fig. 2. Influence of high temperature on pore volume of HPCP PPF0.

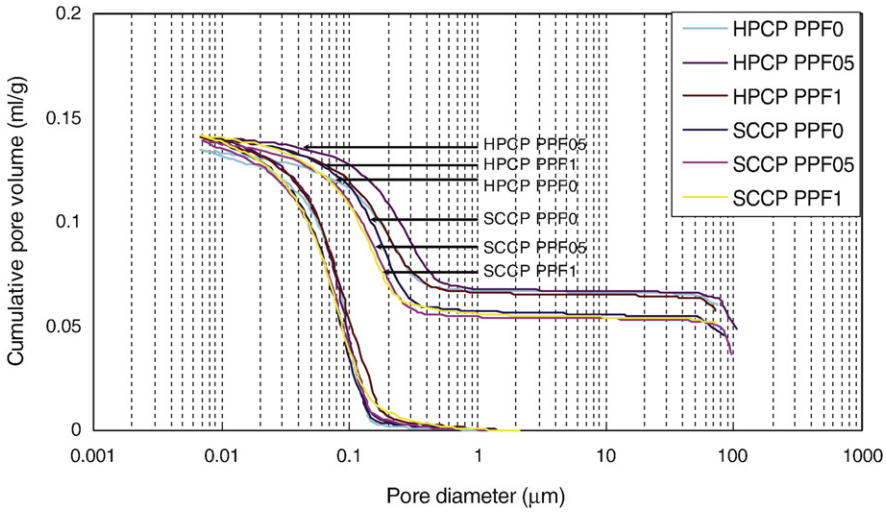

Fig. 3. Cumulative pore volumes after exposure to 200 °C.

The target temperatures chosen were related to the thermal properties of the fibers, the thermal analysis of the components [22], and the possible spalling temperature. The following temperatures were used:

1. 130 °C, range from 100 °C to 130 °C corresponding to the evaporation of adsorbed water;
2. 200 °C, temperature level a little above the melting temperature of PP fiber (171 °C) and the release of hydrated water;
3. 300 °C to 400 °C, temperature interval in which spalling can occur and gel water is released;
4. 500 °C, temperature representing the decomposition of portlandite.

After the target temperature was reached, the samples were kept in the oven for at least 8h to ensure a steady temperature inside. Afterwards, the samples were cooled down to about 105 °C and stored in a dessicator to prevent rehydration. Finally, the temperature decreased to 20 °C and the specimens were unsealed for further testing.

2.3. Mercury intrusion porosity

Numerous researchers have reported the limitation of MIP used for the determination of the microstructure of cementitious materials [23–25]. However, as pointed out by Diamond [26], MIP is so far the most widely used method for determining the pore structure of cement-based materials, not because it "fits" the system best, but because it is the only available procedure that purports to cover nearly the whole range of sizes that must be tallied.

When the pores are considered as cylindrical shape, the radius of the mercury equals the radius of a pore. The relation

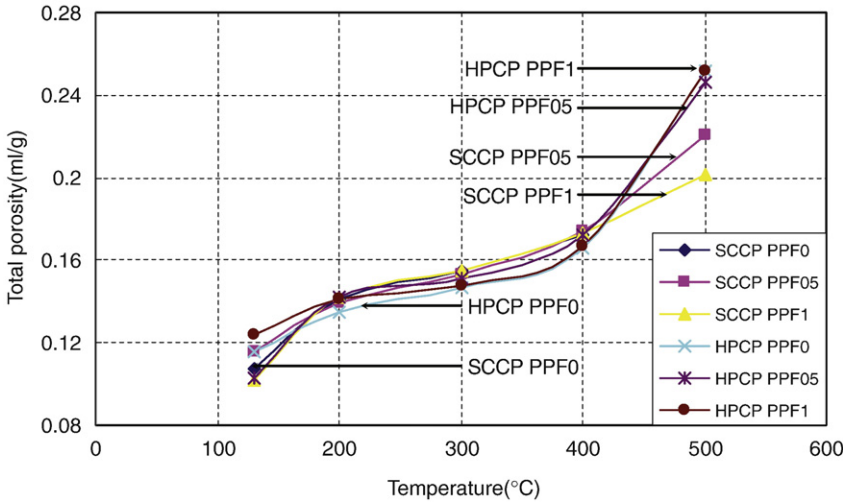

Fig. 4. Development of total porosity with temperature.

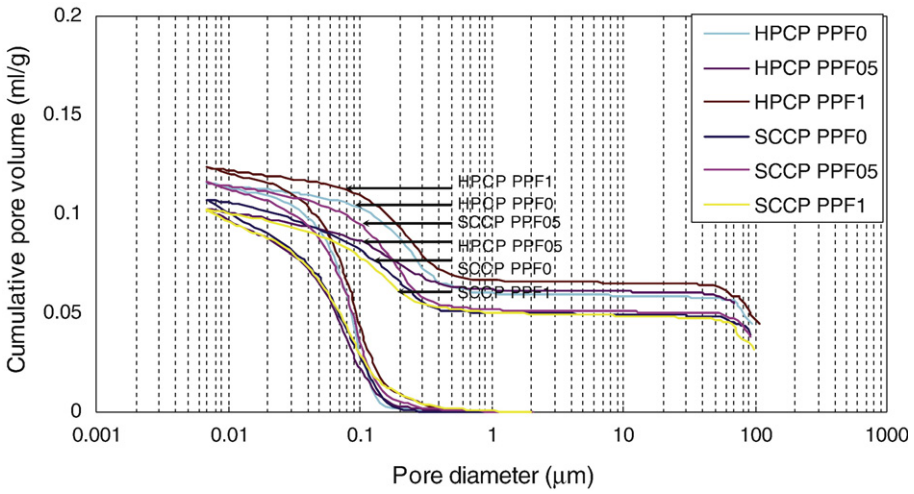

Fig. 5. Cumulative pore volumes after exposure to 130 °C.

between pressure P and the pore radius r can be described by the Washburn equation:

$$P = -\frac{2\sigma \times \cos\theta}{r} \quad (1)$$

where, σ is the surface tension and θ is the contact angle of the mercury to the material tested. In this study, the surface tension of mercury is 480×10^{-3}N/m and the contact angle was 140°.

In this study, a PMI automated porosimeter was used. The maximum pressure of the PMI automated porosimeter is 420MPa. In order to avoid the influence of higher pressures damaging the C–S–H gel structure, the highest pressure used in this experiment was 212MPa. According to the Washburn equation, this pressure could access a minimum pore diameter of 0.0069μm. During the investigation, the sample was removed and split into small pieces of about 1cm^3.

2.4. Backscattered electron microscopy

The scanning electron microscopy was used to determine the microstructure and the phase distribution of samples before and after heating at high temperatures.

In order to obtain a high quality image from the backscattered electron detector, the samples have to be prepared carefully so that the surface is flat. Thus epoxy impregnation, cutting, grinding and polishing, as described in [15], are necessary. A brief description is given in the next paragraph.

The epoxy chosen for impregnation was a very low viscosity epoxy–resin. The sample, weighing around 20g, was collected into a plastic mould, and exposed to vacuum of 30mbar for 1h. The epoxy was fed till the upper face of the sample was covered with epoxy. The impregnated sample was cured at atmospheric pressure at 35 °C for 24h. The cured specimen was cut horizontally from the bottom of the sample mould with a 1mm thick diamond saw. After cutting, the sample was carefully

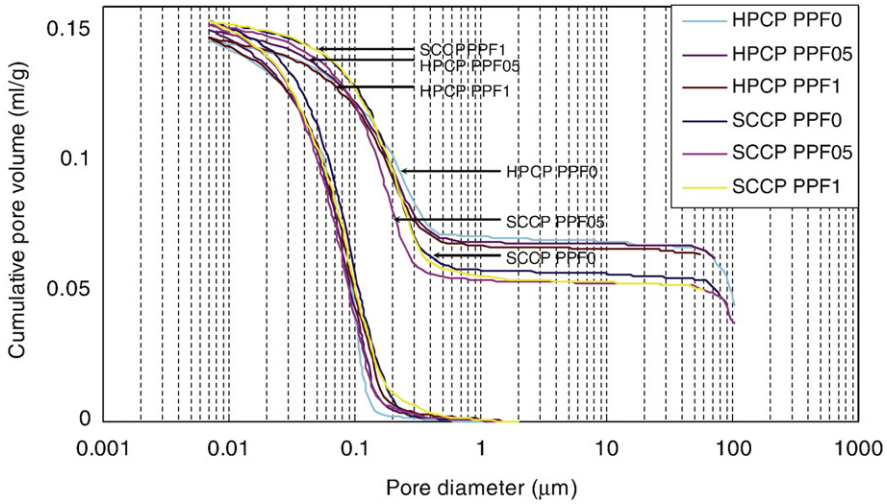

Fig. 6. Cumulative pore volumes after exposure to 300 °C.

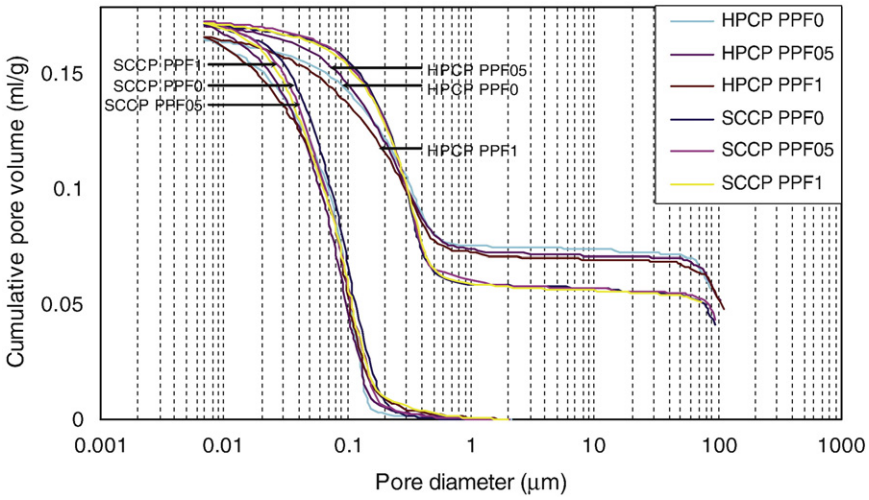

Fig. 7. Cumulative pore volumes after exposure to 400 °C.

ground by hand at moderate pressure on the middle-speed lap wheel with p320, p500 and p1200 sand papers. Polishing was done on a lap wheel with 6, 3, 1, and 0.25μm diamond pastes for about 2min each. The final polishing was carried out on a lap wheel covered with a low-relief polishing cloth.

The images were obtained in an Environmental Scanning Electron Microscope (ESEM) water vapor mode with pressure of 0.1Torr. In order to get a high contrast image for image analysis, an acceleration voltage around 20kV was used. The physical size of the region in each image is 263μm in length and 186μm in width when a magnification of 500X was used. The image size is 1728×1027pixels, so the resolution is 0.152μm per pixel.

A video microscope was also used to take pictures after the specimens were heated to the predicted temperatures. The magnification was 35X and the image size is 640×414 pixels.

2.5. Gas permeability test

Gas permeability measurements were performed with a constant-head permeameter [27]. During testing, dry oxygen was injected from the bottom through laterally confined cylindrical samples. The lateral confinement was 7bars. Gas flow rates were measured with bubble flowmeters.

The effective gas permeability (k_g^{eff}, m^2) is calculated with Darcy's law as modified by the Hagen-Poiseuille relation when the gas flow is assumed to be laminar and unidirectional.

$$k_g^{\text{eff}} = \frac{2\mu_g L P_2 Q}{A\left(P_1^2 - P_2^2\right)} \tag{2}$$

where Q is the gas flow rate measured at pressure P_2 (m^3/s); L and A are the specimen height (m) and cross section (m^2), respectively; μ_g is the dynamic viscosity of the gas ($kg/(m \cdot s)$); P_1 is the absolute inlet pressure (Pa) and P_2 is the outlet pressure (Pa).

3. Results and discussion

3.1. Explosive spalling

When the samples SCCP PPF0 were heated, explosive spalling was clearly heard during the time period when the specimens were kept at 500 °C. Spalling occurred on all

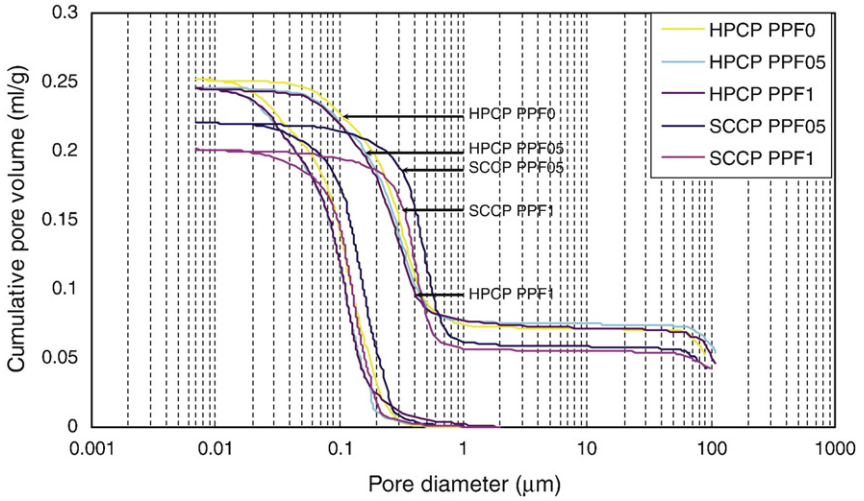

Fig. 8. Cumulative pore volumes after exposure to 500 °C.

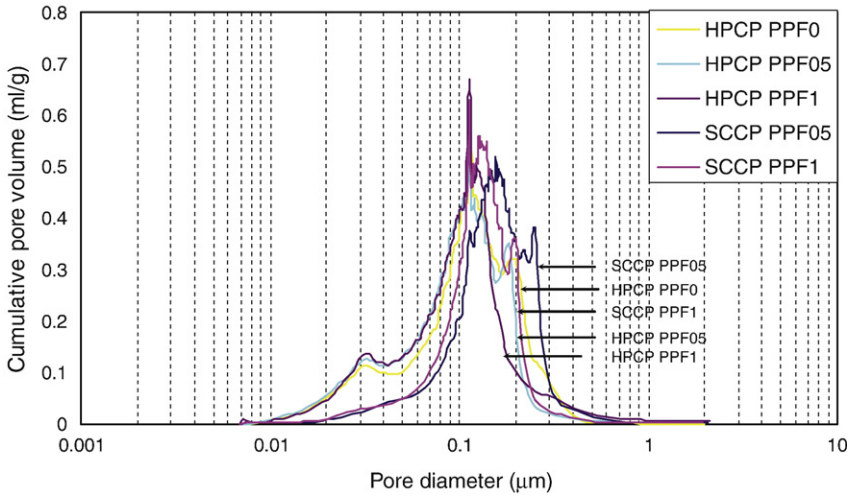

Fig. 9. Absolute pore volumes after exposure to 500 °C.

surfaces since all the faces were heated. This spalling was observed on all specimens for the same mixtures under the same heating conditions.

At the same heating conditions, the SCCP samples with fibers did not show any spalling. No spalling was found for the HPCP samples with or without fibers. Instead, large surface cracks were observed.

3.2. Development of pore structure at different temperatures determined by MIP

With increasing temperatures, the decomposition of hydrated products can be seen from TGA result [28]. The dehydration and the decomposition will lead to a change of the microstructure with increasing heating temperature. The influence of different heating temperatures and mix compositions on the pore structure, as measured by MIP, is shown in Figs. 1–9. Fig. 1 shows a typical MIP result of HPCP without PP fibers. From this figure, it can be seen that with increasing temperature, the total porosity increases as well. The biggest change of the total porosity occurred at 500 °C, when porosity increased to about 1.5 times of that at 400 °C. From TGA measurements [28], the portlandite begins to decompose around 450 °C, and then the pore structure becomes loose, which leads to an increase of total pore volume.

Fig. 2 shows the rate of pore diameter change for different temperatures. It is found that in the temperature range from 130 to 400 °C, the threshold diameter (diameter for which a curve reaches a maximum) does not change significantly and that each curve shows two peaks. However, the peak rate at the threshold diameters increases with increasing temperatures. As shows by TGA [28], from 130 to 400 °C, the main change inside the material is due to release of water, when the adsorbed water, hydrated water and gel water will vaporize with increasing temperature. Simultaneously, the decomposition of the C–S–H and the carboaluminate hydrate only happen to a low extent at this temperature range. Thus the pore structure is characterized by a similar threshold diameter, but by different pore volumes at the threshold diameter.

When the temperature reaches 500 °C, a high pore volume can be observed as shown in Fig. 1, which caused by the decomposition of portlandite. The corresponding curve in Fig. 2 shows three peaks, while the others only have two. At the same time, the threshold diameter increases too.

Fig. 3 shows the cumulative pore volume for all mixtures exposed to 200 °C, as obtained by MIP. Similar pore volume and pore size distribution can be found for all samples, even with different PP fiber contents.

To identify the pore volume change from 130 °C to 200 °C, Fig. 4 shows the total porosity for the mixtures at 130 °C and 500 °C. As expected, the porosity becomes higher with the increase of temperatures. However, the volume change between 130 °C to 200 °C doesn't show the influence of addition of PP

Table 4
Total porosity and threshold diameter as a function of temperature for all mixes

	Total porosity(ml/g)					Threshold diameter (μm)				
Temperature(°C)	130	200	300	400	500	130	200	300	400	500
SCCPPPF0	0.1074	0.1414	0.1547	0.1724	–	0.0792	0.0965	0.0967	0.1069	–
SCCP PPF05	0.116	0.139	0.1534	0.1739	0.2208	0.0932	0.0887	0.0784	0.0948	0.1556
SCCP PPF1	0.1019	0.1418	0.1545	0.1733	0.2015	0.0931	0.0788	0.0932	0.1065	0.1131
HPCP PPF0	0.1156	0.1345	0.1471	0.1661	0.2518	0.0938	0.1031	0.1101	0.112	0.1144
HPCP PPF05	0.1026	0.1418	0.1511	0.1725	0.246	0.0896	0.0993	0.0824	0.0903	0.113
HPCP PPF1	0.1237	0.141	0.1479	0.167	0.252	0.0866	0.0865	0.0888	0.0964	0.1134

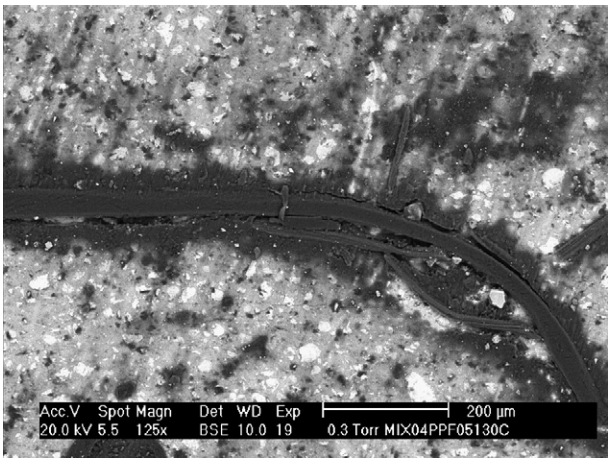

Fig. 10. Image taken from a sample of HPCP PPF05 heated at 130 °C.

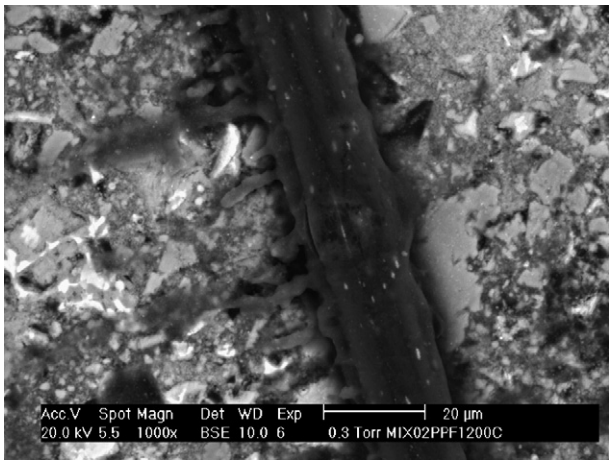

Fig. 12. Image taken from a sample of SCCP PPF1 heated at 200 °C.

fibers. From Figs. 3 and 4, it can be further concluded that the melting of PP fibers does not offer a big increase in pore volume. This is valid both for SCCP and HPCP samples. As mentioned, the PP fiber contents by volume are 0.75% and 1.5% respectively, which is relatively small compared to the total porosity of 14.1% for SCCP PPF0 at 200 °C. There is still discussion on the role of fibers after melting. Quite often it is considered that the melted fibers can offer more absolute space for the escaping moisture vapor. However, from the experiments, no significant additional space has been found after melting at 200 °C. The curves in Fig. 3 show that SCCP and HPCP have similar total porosity even with different PP fiber contents and different w/p ratio.

Similar results within the temperature range from 130 °C to 400 °C can be found for both SCCP and HPCP samples as shown in Figs. 5–7.

Table 4 gives an overview of the total porosity and threshold diameter for all mixtures at different temperatures. It can be seen that for temperatures below 400 °C, the fiber content does not significantly influence the total porosity and threshold diameter, even not above the melting point of the PP fibers, at 171 °C. In Fig. 4, the tendency is similar for all the mixtures.

However, when the samples were heated up to 500 °C, a different phenomenon can be found as illustrated in Fig. 8. With the increase of the total amount of PP fibers, the total porosity decreases significantly. This is different from the findings when the samples were heated within the temperature range below 400 °C, where the amount of PP fiber showed no big influence on the porosity. It is not completely clear why the pore structure changes so pronouncedly when the samples are heated up to 500 °C. A possible reason could be the result of decomposition of hydration products on the one hand, and of the enlargement of the pores or the generation of cracks due to the inner pore pressure on the other hand. After the fibers have melted, the remaining channels will connect the originally isolated pores. Air and moisture can easily get out from inside of the samples. Consequently, the inner pore pressure should decrease and the samples should be less damaged. This hypothesis will be further evaluated by means of gas permeability tests as discussed later.

Fig. 9 shows the relation between the pore diameter and pore volume after exposure to 500 °C for the samples with different

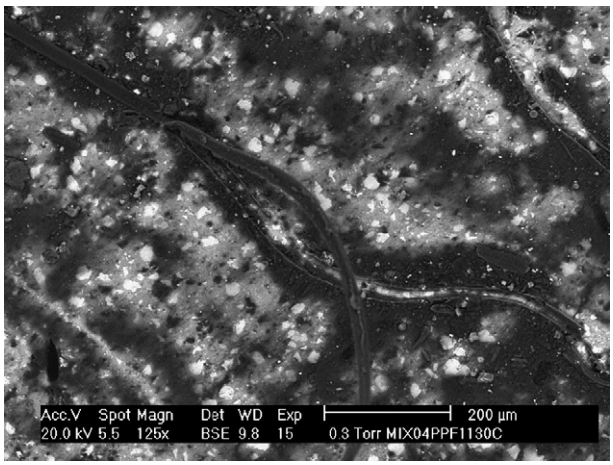

Fig. 11. Image taken from a sample of HPCP PPF1 heated at 130 °C.

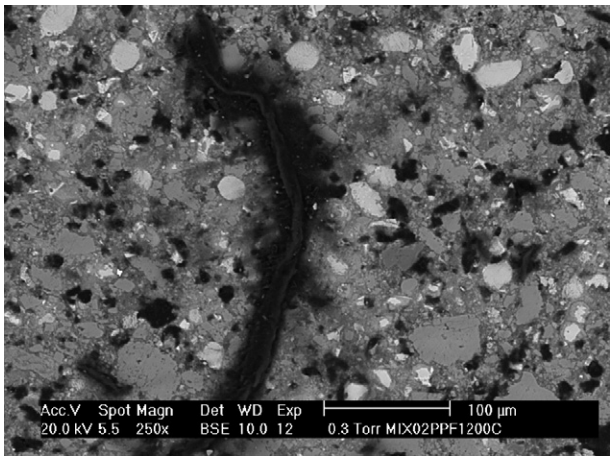

Fig. 13. Image taken from a sample of SCCP PPF1 heated at 200 °C.

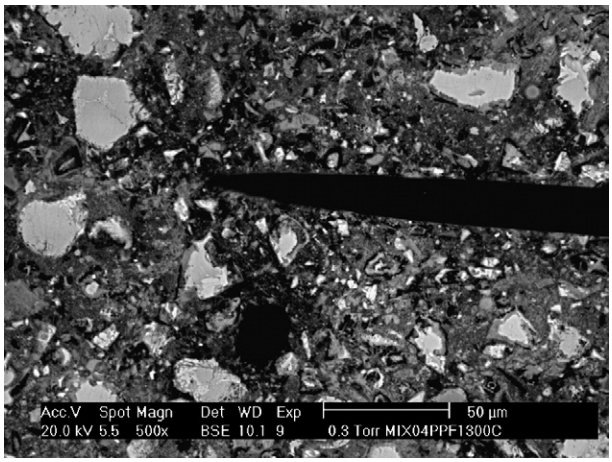

Fig. 14. Image taken from a sample of HPCP PPF1 heated at 300 °C.

PP fiber contents. The result of SCCP PPF0 at 500 °C is not presented because at this temperature spalling happened.

It can be found from Fig. 9, that with the increasing amount of PP fibers, the threshold diameter decreases. Also, the pore volume for larger diameters decreases too. In other words, the more PP fibers are present, the less damage of concrete can be found at this temperature.

3.3. Morphology of PP fibers and micro cracking at different temperatures

Although PP fibers are widely used as an effective method to prevent spalling, the direct evidence showing its physical change is scarce. In this investigation, images of the samples after exposure to different temperatures were obtained by examination of polished sections in an ESEM.

Figs. 10 and 11 were taken from the samples heated at 130 °C; the PP fiber did not melt at this temperature. It can be seen that the PP fibers have a good contact with the hydration products; no obvious interface exists between PP fibers and matrix.

The images of the melting PP fibers shown in Figs. 12 and 13 were taken from the samples heated at 200 °C. When the PP fibers melt, the melted fibers, which are in liquid state, pass through the pores around them. This movement will break the connection among hydrated products. With higher temperature, the melted PP fiber will absorb more energy and vaporize. Thus, the remains of fibers (the fiber channels) and the flow path are connected with each other and form a more connective pore network.

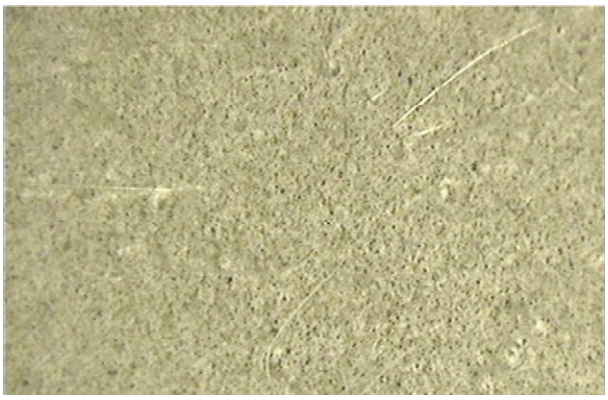

Fig. 16. Image taken from a sample of HPCP PPF1 heated at 130 °C with magnification 35X.

Fig. 14 shows the image taken from a sample of HPCP PPF1 heated at 300 °C. As mentioned above, through melting of PP fibers, the remaining of PP fibers offer a channel for moisture to diffuse. Thus, after melting of the PP fiber, the area near the fiber looks much looser than that without fiber. This phenomenon was studied and verified by three dimensional tomography tests [29].

It is also found that micro cracking showed a higher occurrence at 300 °C than at 130 °C and 200 °C for samples without the addition of PP fiber. Fig. 15 shows some typical cracks from HPCP PPF0 heated at 300 °C. The width of the crack shown in Fig. 15 is about 3µm and the crack goes across the whole image (magnification of 500X). As mentioned before, the minimum pore diameter reachable within the MIP test is 0.0069µm. So, this kind of micro crack (3µm wide) could be captured by the MIP tests.

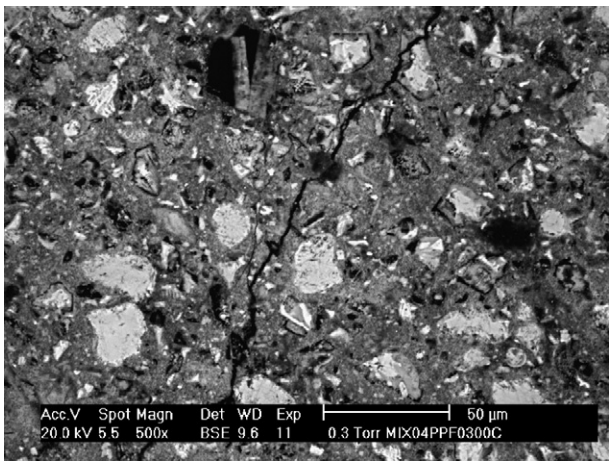

Fig. 15. Image taken from a sample of HPCP PPF0 heated at 300 °C.

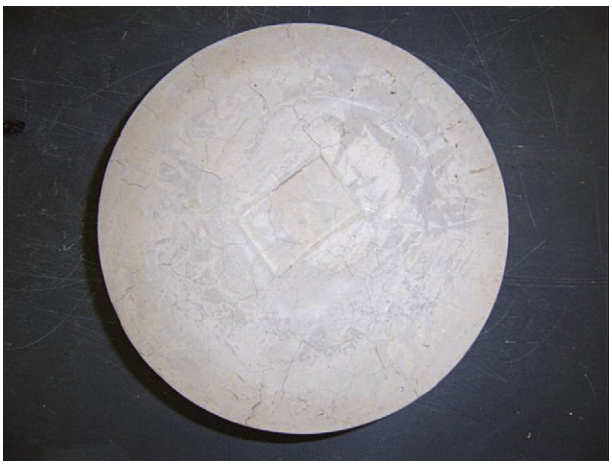

Fig. 17. Image taken from a sample of HPCP PPF0 heated at 400 °C.

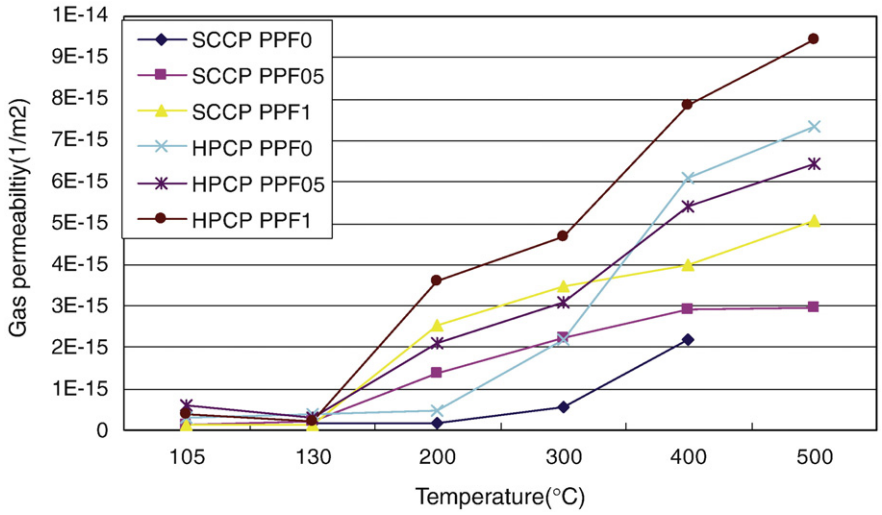

Fig. 18. Gas permeability for the mixtures at 1.5 bars after exposure to high temperatures.

After a reduction of the magnification to 35X (Fig. 16), macro cracks cannot be captured on the surfaces any more, while the PP fibers are still visible.

A typical phenomenon for all the specimens is the visible cracks on the surface, which is showed in Fig. 17. These cracks are regularly radiant and can be qualified as thermal cracks caused by temperature differences.

3.4. Gas permeability

From Fig. 18, it can be found that the value of gas permeability of all samples at 130 °C is almost the same. The gas permeability increases with the increase of exposed temperature. An increase in the gas permeability was found for the samples heated at 200 °C, when the PP fibers were melted. The higher the PP fiber content, the more the gas permeability increases.

Fig. 19 shows the normalized gas permeability, relative to the samples heated at 130 °C. There is almost no change for the samples without PP fiber before 200 °C, as can be observed from the gas permeability for the samples SCCP PPF0 and HPCP PPF0 heated at 130 °C and 200 °C. However, for the samples with PP fibers heated at 200 °C a significant increase on the permeability can be observed. The amount of PP fibers shows great influence on the gas permeability after its melting point. For the same fiber content, the increase of gas permeability is at the same level for the different mixes. The gas permeability of the samples with PP fiber content of 1kg/m³ is almost twice as high as for the samples with PP fiber content of 0.5kg/m³.

The role of PP fiber can be seen more clearly when taking the gas permeability at 200 °C as reference, as shown in Fig. 20. From this investigation, there are at least two different factors which affect the gas permeability after heating. For the samples without PP fibers, a big increase of gas permeability starts at 300 °C. Cracking may be considered as the reason for the gas permeability increase. As mentioned above, the ESEM test showed a higher occurrence of micro cracking 300 °C for

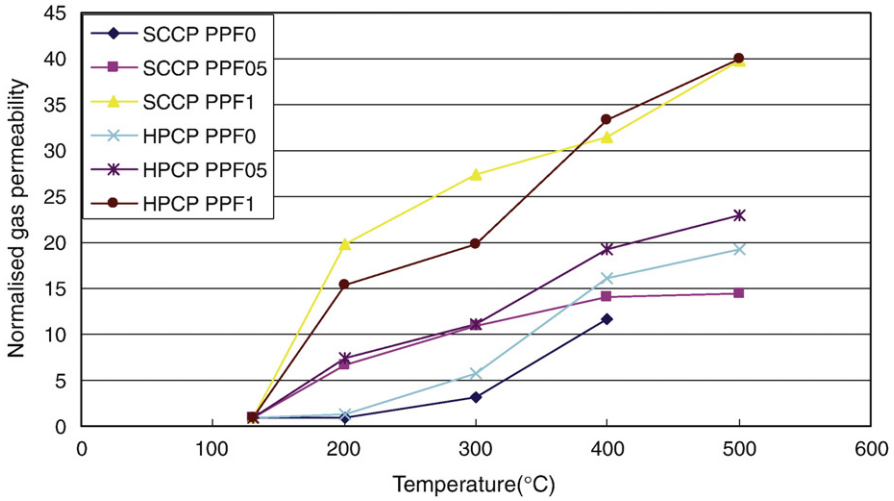

Fig. 19. Normalized gas permeability, relative to the samples heated at 130 °C.

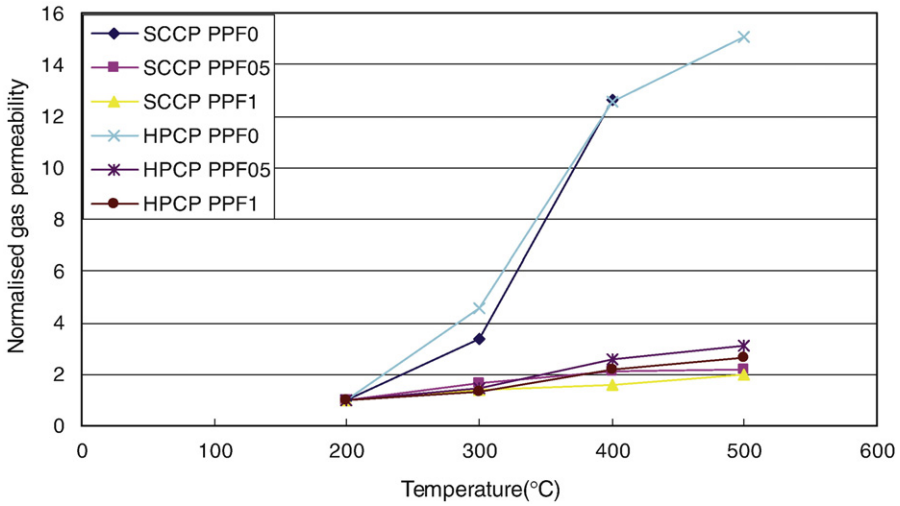

Fig. 20. Normalized gas permeability, relative to the samples heated at 200 °C.

samples without the addition of PP fiber. While for the samples with PP fiber, there is no doubt that the melted PP fibers are the major reason for the change of gas permeability, for it is found the formation of connected channels from ESEM observation. Obviously from Fig. 20, the gas permeability is more influenced by the presence of PP fibers rather than the surface cracking.

Fig. 21 shows the normalized gas permeability, relative to the mixtures without PP fibers.

From Fig. 21, the influence of PP fibers can be seen explicitly. The normalized gas permeability increases significantly at 200 °C. The higher the fiber content, the more the gas permeability increases. The influence of PP fibers is more obvious for SCCP than for HPCP. A PP fiber content of 0.5 kg/m³ in SCCP shows a similar effect as for a fiber content of 1 kg/m^3 in HPCP. After heating up to 200 °C, the normalized gas permeability for the mixtures with PP fibers tends to decrease. After 400 °C, the normalized gas permeability results are on the same level. The normalized curves show that the melted fibers can improve the gas permeability significantly near the melting point. After this point, the increasing tendency slows down, as the gas permeability is then also influenced by other factors, such as micro cracks, as discussed previously.

3.5. Discussion about the relation between the development of microstructure and gas permeability

In reference [28], a good correlation was found between the gas permeability coefficient and the measured pore size using a MIP method. However, when PP fibers are added to concrete, the suggested relationship seems to meet some obstructions, as the total porosity and threshold diameter for concrete with and without PP fibers are not significantly different below 500 °C, while the gas permeability with PP fibers shows a clear increase after 130 °C. The total porosity and threshold diameter even

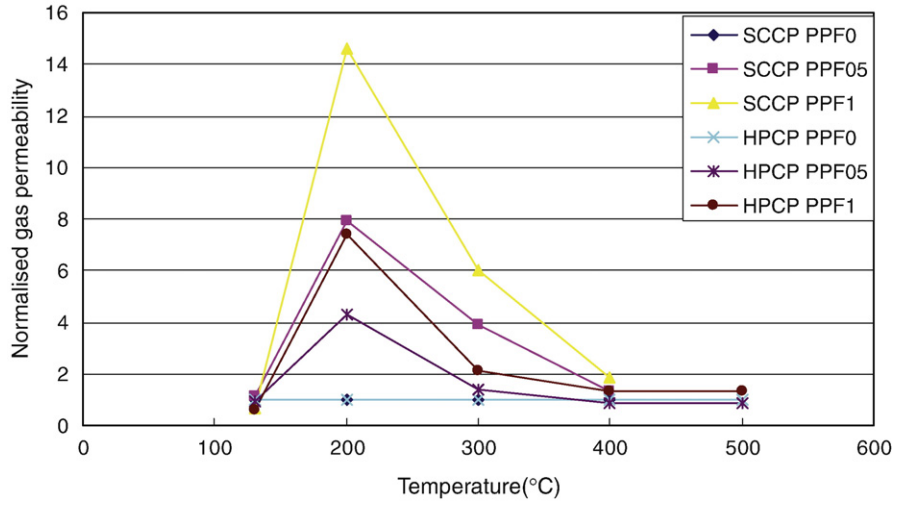

Fig. 21. Normalized gas permeability, relative to the samples without PP fiber.

decreased at 500 °C. It seems that only two representative parameters are not enough to describe the gas permeability after fire.

Since the gas permeability indicates the easiness of the gas transport, it is also related to the micro pore structure. As mentioned above, no big difference exists in pore volume for the mixtures with or without fibers. However, it can be deduced that the connectivity of the pores is improved by the melting of the PP fibers. This connectivity is a major factor influencing gas permeability. The images from BSE, as shown before, show the increased connectivity to some extent.

From the normalized gas permeability relative to the samples heated at 200 °C (in Fig. 20), the concrete without PP fiber showed a large increase on permeability after heating up to 300 °C, while those without PP fibers did not show relevant changes. As shown in Fig. 15 taken from a sample of HPCP PPF0, fine cracks occur more often, and offer additional channels for gas escape. A similar result was also reported in reference [30].

The connectivity of the pores is the major factor which determines the gas permeability. The original isolated pores become connected when the PP fibers melt with increasing temperature. In this way, the connectivity is improved significantly. After 300 °C, with the occurrence of more fine cracks, the connectivity will be further improved. This is also verified by three dimensional tomography tests [29].

However, up to now all these phenomena can only be described qualitatively. Some numerical models have to be developed based on the microstructure analysis, in order to explain the influence of connectivity on transport properties in more detail.

4. Conclusions

Based on the experimental results, the following conclusions can be drawn concerning the influence of high temperatures on the microstructure and the permeability of SCCP and HPCP, and its relation to spalling.

1. At elevated temperatures of 400 °C, hydrated water inside the concrete was released, leading to microstructural changes. From the investigation from SCCP and HPCP, the threshold pore diameter did not change significantly. However the pore volume at the threshold diameter and the total pore volume increased.
2. The melting fibers can be absorbed by the surrounding pores. The total porosity does not show a significant change due to the melting of the PP fibers. This is valid both for SCCP and HPCP.
3. The connectivity of the pores will be greatly influenced by the melting of the PP fibers. This finding is supported by BSE image analysis and gas permeability tests. Damage caused by high temperature can be avoided, due to the increased pore connectivity after melting of the PP fibers.
4. The connectivity of pores and micro cracks are the major factors which determine the gas permeability in high temperatures. Furthermore, the connectivity of the pores acts as a dominant factor for temperatures below 300 °C. This is more pronounced in SCCP samples. For higher temperatures, micro cracks should be becoming the major factor influencing the gas permeability.

Acknowledgement

The research was financially supported by the Fund for Scientific Research-Flanders (Belgium) (FWO), which is gratefully acknowledged. The technical support during MIP measurements from the company PMI (Porous Materials, Inc.) is also appreciated.

References

[1] J.R. Lawson, L.T. Phan, F. Davis, Mechanical Properties of High Performance Concrete After Exposure to Elevated Temperature, NISTIR 6475.
[2] Patrick J.E. Sullivan, A probabilistic method of testing for the assessment of deterioration and explosive spalling of high strength concrete beams in flexure at high temperature, Cement and Concrete Composites 26 (2004) 155–162.
[3] Faris Ali, Outcomes of a major research on fire resistance of concrete columns, Fire Safety Journal 39 (2004) 433–445.
[4] K.D. Hertz, Limits of spalling of fire-exposed concrete, Fire Safety Journal 38 (2003) 103–116.
[5] B. Persson, Fire resistance of self-compacting concrete, SCC, Materials and Structures 37 (273) (2004) 575–584.
[6] Z.P. Bazant, M.F. Kaplan, Concrete at high temperatures, Longman – Addison-Wesley, London, 1996.
[7] P. Kalifa, F.D. Menneteau, D. Quenard, Spalling and pore pressure in HPC at high temperatures, Cement and Concrete Research 30 (12) (2000) 1915–1927.
[8] P. Kalifa, Gregoire Chene, Christophe Galle, High-temperature behaviour of HPC with polypropylene fibres From spalling to microstructure, Cement and Concrete Research 31 (2001) 1487–1499.
[9] P. Kalifa, M. Tsimbrovska, V. Baroghel-Bouny, High performance concrete at elevated temperatures — an extensive experimental investigation on thermal, hygral, and microstructural properties, in: P.C. Aitcin, Y. Delagrave (Eds.), Proceedings of the International Symposium on High-Performance and Reactive Powder Concrete Sherbrooke '98, vol. 2, 1998, pp. 259–279.
[10] Gray R. Consolazio, Michad C. MeVay, Jeff W. Rish, Measurement and prediction of pore pressure in cement mortar subjected to elevated temperature, International Workshop on Fire Performance of High-Strength Concrete, NIST, Gaithersburg MD, February 13-14,1997, Proceedings, 1997.
[11] Izabela Hager, Pierre Pimenta, The impact of the addition of polypropylene fibers on the mechanical properties of high performance concretes exposed to high temperatures, proceedings of BEFIB, Lyon (France), 2004, September.
[12] A. Noumowe, Mechanical properties and microstructure of high strength concrete containing polypropylene fibres exposed to temperatures up to 200 °C, Cement and Concrete Research, article, 2005.
[13] B. Persson, Mitigation of fire spalling of concrete with fibers, Presentation in technical committee "Durability of Self-Compacting Concrete", Ghent (Belgium), April 2005.
[14] G. Ye, Experimental study and numerical simulation of the development of the microstructure and permeability of cementitious materials, PhD thesis, Delft University of technology, Delft, 2003.
[15] A.J. Katz, A.H. Thompson, Quantitative prediction of permeability in porous rock, Physical Review. B 34 (1986) 8179–8181.
[16] E.J. Garboczi, J.G. Berryman, Elastic moduli of a material containing composite inclusions: effective medium theory and finite element computations, Mechanics of Materials 33 (8) (2001) 455–470.
[17] C.J. Haecker, D.P. Bentz, X.P. Feng, P.E. Stutzman, Prediction of cement physical properties by virtual testing, Cement International 1 (3) (2003) 86–92.
[18] Dale P. Bentz, Fibers, Percolation, and Spalling of High-Performance Concrete, ACI materials journal, 2000, pp. 351–359, may-June.

[19] D. Gawin, F. Pesavento, B.A. Schrefler, Modelling of hygro-thermal behaviour of concrete at high temperature with thermo-chemical and mechanical material degradation, Comput. Methods Appl. Mech. Engrg. 192 (2003) 1731–1771.
[20] G.L. England, N. Khoylou, Moisture flow in concrete under steady state non-uniform temperature states-experimental observations and theoretical modeling, Nuclear Engineering and Design 156 (1995) 83–107.
[21] R.T. Tenchev, J.A. Purkiss, L.Y. Li, Numerical analysis of thermal spalling in a concrete column, 9th National Congress on Theoretical and Applied Mechanics, Bulgaria, Varna, 2001, pp. 19–22, Sept.
[22] G. Ye, X. Liu, G. De Schutter, A.M. Poppe, L. Taerwe, Influence of limestone powder used as filler in SCC on hydration and microstructure of cement pastes, Cement and Concrete Composites 29 (2) (2007) 94–102.
[23] S. Diamond, Mercury porosimetry: an inappropriate method for the measurement of pore size distribution in cement-based materials, Cement and Concrete Research 30 (10) (2000) 1517–1525.
[24] R.A. Olson, C.M. Neubauer, H.M. Jennings, Damage to the pore structure of hardened Portland cement paste by mercury intrusion, Journal of American Ceramic Society 80 (9) (1997) 2454–2458.
[25] R.A. Cook, K.C. Hover, Mercury porosimetry of hardened cement pastes, Cement and Concrete Research 21 (6) (1999) 933–943.
[26] S. Diamond, Methodologies of PSD measurement in HCP: postulates, peculiarities, and problems, Proc. Material Research Society Symposium, Pore structure and permeability of cementitious materials, vol. 137, 1988, pp. 83–92.
[27] RILEM TC 116-PCD: permeability of concrete as a criterion of its durability, B: measurement of the gas permeability of concrete by Rilem–Cembureau method, Materials and Structures vol. 32 (1999) 174–179.
[28] G. Ye, X. Liu, G. De Schutter, L. Taerwe, Phase distribution and microstructural changes of self-compacting cement paste at elevated temperature, Accepted by Cement and Concrete Research 2007, on line.
[29] G. Ye, G. De Schutter, L. Taerwe, K. van Breguel, The effect of pp fiber on the compressive strength and permeability of self-compacting concrete and high performance concrete, proceeding of Knud Hojgaard Conference on Advanced Cement-based Materials: Research and Teaching, Lyngby, Denmark, 2005, pp. 205–214, 12-15 June.
[30] C. Galle, J. Sercombe, Permeability and pore structure evolution of silicocalcareous and hematite high-strength concretes submitted to high temperatures, Materials and Structures 34 (2001) 619–628.